Proc. Natl. Acad. Sci. USA
Vol. 85, pp. 6954–6958, September 1988
Medical Sciences

Anoxic contractile failure in rat heart myocytes is caused by failure of intracellular calcium release due to alteration of the action potential

(excitation–contraction coupling/ischemia/oxygen/hypoxia)

MICHAEL D. STERN*†, HOWARD S. SILVERMAN*†, STEVEN R. HOUSER‡, RICHARD A. JOSEPHSON*†, MAURIZIO C. CAPOGROSSI*†, COLIN G. NICHOLS§, W. JONATHAN LEDERER§, AND EDWARD G. LAKATTA*†§

*Laboratory of Cardiovascular Science, Gerontology Research Center, National Institute on Aging, National Institutes of Health, Baltimore, MD 21224; †Division of Cardiology, Johns Hopkins University School of Medicine, 600 North Wolfe Street, Baltimore, MD 21205; ‡Department of Physiology, Temple University School of Medicine, Philadelphia, PA 19140; and §Department of Physiology, University of Maryland School of Medicine, Baltimore, MD 21201

Communicated by J. Edwin Seegmiller, May 25, 1988 (received for review February 5, 1988)

ABSTRACT **Anoxia of the heart causes failure of contraction before any irreversible injury occurs; the mechanism by which anoxia blocks cardiac excitation–contraction coupling is unknown. Studies in whole muscle are confounded by heterogeneity; however, achieving the low oxygen tensions required to study anoxia in a single myocyte during electrophysiological recording has been a barrier in experimental design. Guided by calculations of oxygen transport, we developed a system to insulate myocytes in an open dish from oxygen by a laminar counterflowing argon column, permitting free access to the cell by microelectrodes while maintaining a Po_2 <0.02 torr (1 torr = 133 Pa). In the absence of glucose, the amplitude of stimulated contraction of anoxic ventricular myocytes fell to zero over 2 min after a lag period attributable to the consumption of endogenous glycogen. The cytosolic calcium concentration transient, measured by indo-1 fluorescence, fell to zero simultaneously with contraction. After the twitch had failed, microinjection of caffeine around the cell still caused a large calcium release and contraction, indicating that sarcoplasmic reticular calcium stores were not depleted. Twitch failure was accompanied by shortening and then failure of the action potential; under voltage clamp, large outward currents, reversing at the resting potential, developed during contractile failure. After failure of action potential-mediated contraction, voltage-clamp depolarization, with a large command voltage to compensate for the series-resistance error due to outward currents, restored normal twitch contraction. We conclude that anoxic contractile failure in the rat myocyte is due to alteration of the action potential and the distal pathways of excitation–contraction coupling remain essentially intact.**

The ischemic heart stops contracting before irreversible damage occurs. A similar effect is seen when the heart is made hypoxic in the absence of glycolytic substrate. Decline of contractile force and a progressive shortening of the action potential duration have also been seen in isolated ventricular muscle (1–4) and cultured embryonic-chicken-heart cell layers (5–7) subjected to substrate-free hypoxia.

The mechanism of contractile failure has been difficult to study in multicellular preparations because of the effects of heterogeneity (8–10) and decreased cell-to-cell electrical coupling during hypoxia (11). To produce hypoxia in a single isolated cell, however, a Po_2 as low as 0.15 torr (1 torr = 133 Pa) must be achieved (12). This experimental level has previously not been feasible (13) because of the basic incompatibility between complete exclusion of atmospheric oxygen, which requires hermetically sealed systems (10), and electrophysiological recording, which requires microelectrode access to the cell.

To solve this problem, we calculated the degree to which atmospheric oxygen could be excluded from an *open* dish by a layer of inert gas. We found that a very high degree of exclusion is possible, provided the inert gas is maintained in a state of laminar flow against the oxygen gradient at a sufficiently high controlled velocity. Based on these calculations, a device was constructed, the laminar counterflow barrier well, with which we have studied excitation–contraction coupling in single anoxic isolated rat ventricular myocytes.

MATERIALS AND METHODS

In our technique, the cell is freely accessible from above but is protected from oxygen by a laminar counterflowing layer of inert gas. The partial pressure of oxygen in a steady laminar flow of gas with vector velocity $v(x)$ is determined by the convective diffusion equation:

$$D\nabla^2 P - v(x)\cdot\nabla P = 0, \quad [1]$$

where D is the diffusion coefficient of oxygen in the inert gas, P is the oxygen pressure, and ∇ is the Laplacian (vector differential) operator. A one-dimensional approximation to the problem, which can be solved analytically, may be obtained by considering a layer of gas rising at constant velocity v in a well of depth L. The Po_2 at the bottom of the well is

$$P_{bottom} = P_{top}\exp(-vL/D). \quad [2]$$

Because of the rapid fall-off of the exponential, extremely low oxygen tensions may be obtained at the bottom of the well, provided sufficiently rapid, steady, and approximately vertical laminar flow can be maintained. By using argon, which at 37°C has 1.3 times the density of room-temperature air, the upwelling gas forms a stable laminar layer under air.

A prototype well was constructed as shown in Fig. 1. Prehumidified 99.9995% argon, regulated at a flow of 235 ml/min, formed a stable horizontal layer (extending 3 mm above the top of the well), which was visualized against cigar smoke. At higher flows the argon formed a dome over the orifice and then broke up into turbulent eddies. From Eq. 2, by use of the diffusion coefficient for oxygen in argon of 0.218 cm^2 per sec at 1 atmosphere (1 atm = 1.013×10^5 Pa) and 37°C (14), the predicted Po_2 at the well bottom is 2×10^{-7} torr. The oxygen pressure measured with a precision gold polarographic electrode (Orbisphere, Geneva) was <0.02 torr, the measurement being limited by leakage of oxygen

The publication costs of this article were defrayed in part by page charge payment. This article must therefore be hereby marked "*advertisement*" in accordance with 18 U.S.C. §1734 solely to indicate this fact.

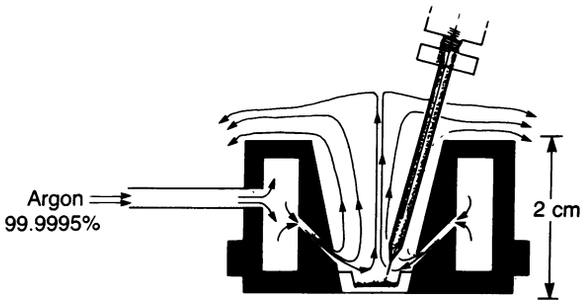

FIG. 1. The laminar counterflow barrier well, shown schematically in cross-section. Ultra-pure argon at a controlled flow rate enters the conical well from a toroidal manifold through a circumferential array of small holes, two of which are seen in cross-section, establishing a roughly vertical laminar flow, in which oxygen tension diminishes exponentially in the counterflow direction. The bottom of the well is a precision quartz dish 1 cm in diameter and 2 mm in height, in which the cells are studied.

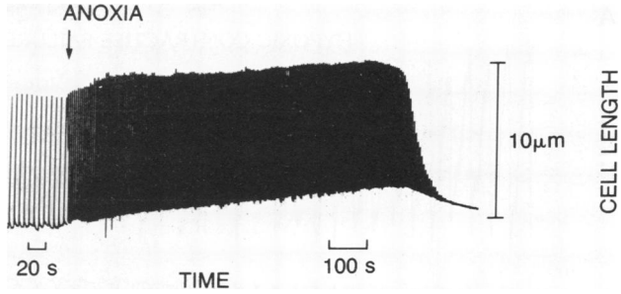

FIG. 2. Contraction amplitude of a rat cardiac myocyte field-stimulated at 0.2 Hz during anoxia. The lag period, during which contraction amplitude *increases* somewhat, followed by a rapid total fall of contractility, are typical. The decrease of diastolic length during the late part of the lag period, followed by relengthening at the time of contractile failure, is representative but usually is more subtle than in this myocyte.

across the fluran gasket used to seal the electrode beneath the well.

In actual operation, a custom-made optical-quality quartz dish 1 cm in diameter and 2 mm deep (Mindrom Precision Products, Cucamonga, CA) formed the bottom of the well. In this dish, adult rat left ventricular myocytes, isolated as described (10), were superfused by glucose-free Hepes buffer (144 mM NaCl/5 mM KCl/1.2 mM $MgSO_4$/10 mM Hepes, pH 7.4) containing 1 mM Ca^{2+} with 0.05 mM octanoate as respiratory substrate, equilibrated with argon (99.9995%), delivered through stainless-steel tubing. The liquid flow was regulated by positive gas pressure in the buffer flask; contact of the liquid with pumps, valves, or plastics was avoided. Outflow from the dish was through platinum-needle tubing, which also served as the anode for field stimulation, so that oxygen produced electrolytically was removed with the effluent.

Twitch amplitude was measured as extent of shortening by video edge-tracking during field stimulation or current-clamp stimulation (rate, 0.2–1 Hz) with the whole-cell patch-pipette technique. Pipettes were 5–10 MΩ borosilicate, filled with 120 mM KCl/10 mM NaCl/5 mM $MgCl_2$/20 mM Hepes, pH 7.2 with KOH. Cytosolic calcium was measured by indo-1 fluorescence in cells preloaded with the acetoxymethyl ester of the dye by the method of Poenie *et al.* (15). The chamber was mounted on a specially modified Zeiss IM-35 epifluorescence microscope, and fluorescence was excited every 5 msec by an 8-μsec flash of light at 350 nm from a pulsed xenon strobe lamp, with synchronous collection of emitted light. The bright-field image of the cell was monitored simultaneously during the interval between flashes with red (650–700 nm) illumination (16).

RESULTS AND DISCUSSION

In contrast to isometric papillary muscles (4), single rat myocytes showed no immediate decrease in contraction amplitude at the onset of hypoxia. A modest *increase* in contraction amplitude associated with a slight decrease in diastolic cell length was typical of the initial hypoxic period. After a lag, which ranged from 3 to 48 min, contraction amplitude began to fall rapidly, whereas diastolic cell length increased (Fig. 2), proceeding to complete contraction failure within 2 min.

Reoxygenation, by simply stopping the flow of liquid and gas phases to permit back-diffusion of oxygen, restored normal contraction within a few heartbeats. A second period of hypoxia resulted in contractile failure in <6 min in all cells. This shortening of the lag period after the first cycle of hypoxia is compatible with the hypothesis that variability of the initial lag period is due to differences in the time required for stored-glycogen consumption.

To test this hypothesis and to exclude the possibility that the lag period was from a delay in the onset of hypoxia, we studied cells pretreated for 1 hr with 10 mM 2-deoxyglucose to inhibit glycogenolysis. When these cells were made hypoxic, their contraction amplitude, which initially had been normal, began to fall within 30 sec of the nominal onset of hypoxia and failed completely within 50 sec; contraction was fully restored within 2–3 heartbeats upon reoxygenation.

The failure of contraction during anoxia might be attributed to failure of myofilament activation because of a depression of the cytosolic calcium transient current, or to unresponsiveness of the myofilaments themselves to calcium. In eight cells loaded with indo-1, the calcium concentration transient fell to zero simultaneously with contraction failure (Fig. 3*A*). Although failure of calcium concentration transient is *a fortiori* sufficient to explain contraction failure, simultaneous alteration of myofilament response could also occur. To examine this point, we plotted the relationship between the peak indo-1 calcium signal and extent of shortening in three cells both during anoxia and during alteration of extracellular calcium before anoxia (Fig. 3*B*). The points for anoxic failing beats fell close to or above the myofilament response curve defined by altering extracellular calcium, indicating that no major depression of myofilament response occurs before failure of the calcium concentration transient.

It has been suggested that the calcium transient might fail because of sarcoplasmic reticular calcium depletion from fall in the free energy of ATP hydrolysis (17). To test this hypothesis, caffeine (10 mM) was rapidly ejected from a micropipette adjacent to the cell, to directly release sarcoplasmic reticular calcium after contractile failure had developed. Ejected volume was limited to an amount that produced no evidence of reoxygenation when caffeine was omitted from the pipette, as determined by control experiments in which caffeine-free oxygenated buffer was ejected from matched pipettes (i.e., pipettes of the same impedance and pulled with the same settings) with the same applied pressure and duration. Caffeine evoked a large contraction (Fig. 4*A*) within <1 sec. The size of the indo-1 calcium transient produced by caffeine after anoxic contractile failure was comparable to that seen before anoxia, whereas contraction amplitude was only modestly reduced (Fig. 4*B*). Therefore, sarcoplasmic reticular calcium depletion is not responsible for contractile failure, and no major alteration of myofilament sensitivity sufficiently accounts for contractile failure.

Alternatively, failure of calcium release might be from alteration of the action potential. In seven cells current-

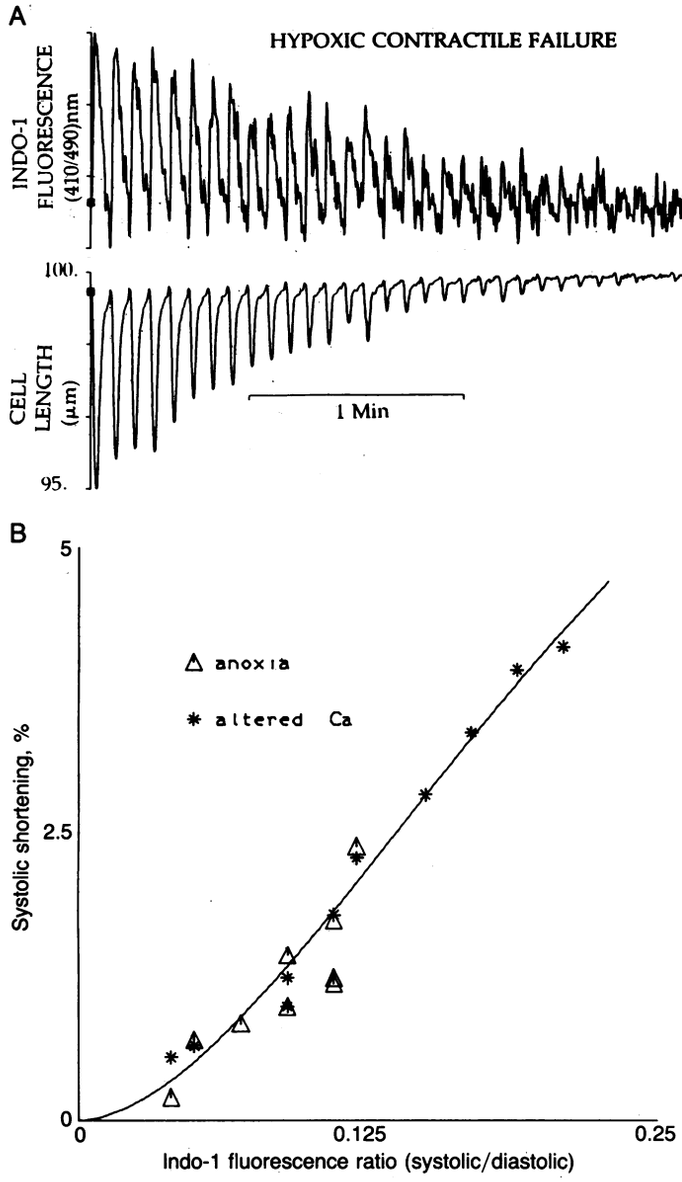

FIG. 3. (*A*) Cytosolic calcium transient currents (measured as ratio of indo-1 fluorescence at 410 nm and 490 nm) and simultaneous cell length (shortening, downward) during the period of contractile failure. The record has been telescoped by omitting the last 4 sec of diastole after each beat to conserve computer memory space. (*B*) Myofilament response, determined by plotting contraction amplitude (% shortening) against amplitude of the indo-1 calcium concentration transient. Control points (*) were obtained by varying extracellular calcium from 2 mM to 0.2 mM during normoxia; the solid curve is the best fit by a Hill equation. The anoxic failing beats (△) from the same cell in constant extracellular 1.0 mM calcium lie along the curve, indicating that myofilament depression makes no major contribution to the decline of contraction. Results in two other cells were similar, except that some of the early anoxic points fell above the curve (i.e., *enhanced* myofilament response during anoxia before contractile failure).

clamped at rates of 0.2–1 Hz, there was little immediate change in resting or action potentials at the *onset* of hypoxia. After a lag period, duration of the action potential began to shorten rapidly from beat to beat (Fig. 5*A*). Once this shortening began, it proceeded to complete inexcitability within 2 min. Resting potential (-75.6 ± 3.7 mV) remained unchanged ($\Delta V = 0.8 \pm 1.0$ mV). Reoxygenation at this time restored a normal action potential within a few beats. When anoxia was continued after electromechanical failure, cells underwent an abrupt contracture to an inert rectangular form (presumed to be a rigor state) after 1–4 min without change of resting potential.

Simultaneous video edge-tracking and electrical recording from four cells showed that action potential shortening and contractile failure coincided (Fig. 5*B*). Under voltage clamp, contractile failure was associated with the rapid development of very large time-independent outward currents, which probably flow through the ATP-inhibited potassium channel (18). The effect of these currents is to clamp the membrane potential near the resting potential.

If anoxic contractile failure is caused by the action potential changes, then voltage-clamp depolarization should restore the contraction. The outward current rapidly becomes too large to permit accurate single-electrode voltage clamp because of series-resistance error. However, by increasing the voltage-clamp command potential to compensate manually for the large voltage drop across the pipette access resistance, we could depolarize the cell 2 min after contractile failure and this, indeed, restored a sizable contraction (Fig. 6).

Our results show that hypoxic contractile failure in the rat myocyte is primarily from shortening and then abolition of the action potential. Because voltage-clamp depolarization can restore normal twitch amplitude, the steps in excitation–contraction coupling that follow the generation of the action potential are probably, at least qualitatively, intact. To evaluate these steps quantitatively, it would be necessary to block the large outward conductance that develops during hypoxia and which is presumably the major cause of the action potential changes. This conductance becomes so large that space-clamp limitations would preclude accurate voltage control, even with a two-electrode voltage clamp. Pending such studies, the explanation that the twitch restored under voltage clamp is triggered by electrogenic sodium–calcium exchange rather than the usual slow inward calcium current cannot be excluded. However, because the command voltage in this experiment is fully accounted for by the estimated voltage drop across the pipette access resistance, probably

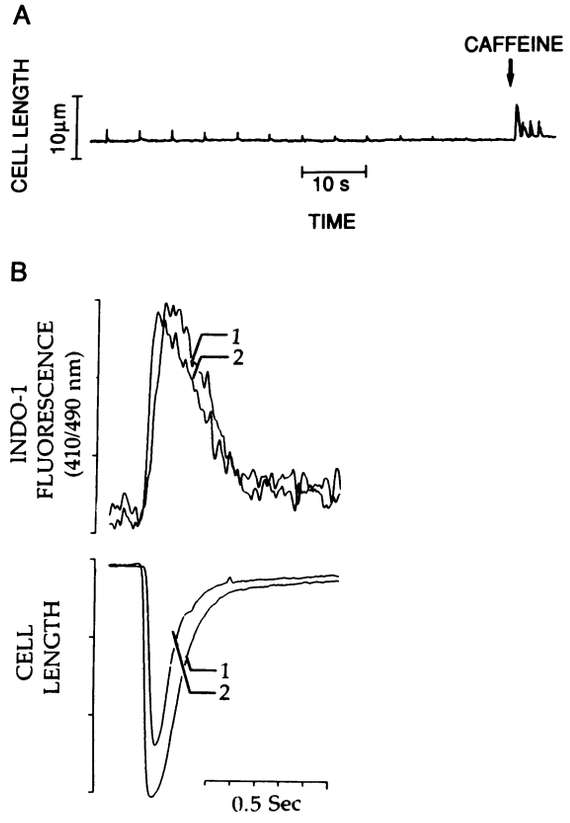

FIG. 4. (*A*) After failure of stimulated contraction during anoxia, a large contraction is produced by caffeine, which directly releases calcium from the sarcoplasmic reticulum, showing that depletion of sarcoplasmic reticular calcium does not cause contractile failure. (*B*) Indo-1 calcium concentration transients and corresponding contractions produced by caffeine before onset of hypoxia (trace 1) and during continued hypoxia after failure of stimulated contraction (trace 2).

the actual depolarization of the cell is modest and does not reach that range in which sodium–calcium exchange is active.

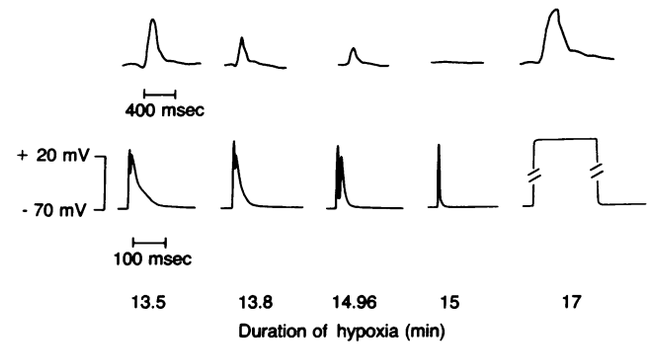

FIG. 6. After 13.5 min of anoxia, the contraction (*Upper* traces) of a current-clamped myocyte failed over 1.5 min, associated with shortening and failure of the action potential (*Lower* traces). Two minutes later, during continued anoxia, contraction was still elicited by a 200-msec voltage-clamp step (*Lower* trace, voltage). The very large outward current, 50 nA, caused an estimated voltage drop of 700 mV across the access resistance, equal to the command potential, so that the exact magnitude of the depolarizing step seen by the cell could not be determined.

The large potassium conductance that develops in hypoxia resembles that seen with metabolic blockade (19, 20) and with direct depletion of ATP by patch-pipette dialysis (20). The K_d of the inactivation of this current by ATP in isolated patches is only 0.1 mM (18), which is more than an order of magnitude below the ATP level present in whole hearts at anoxic contractile failure (4). This fact may indicate a subcellular compartmentalization of ATP. Alternatively, heterogeneity may be intercellular—the large outward conductance of a few cells that are ATP depleted electrotonically shunting intact cells. This situation would be compatible with the large cell-to-cell variability in lag duration that precedes contractile failure and with the heterogeneity in time of ATP depletion found in anaerobic cell suspensions (9). The latter studies showed that substantial ATP depletion precedes structural contracture by 1–6 min, similar to the time elapsing between contractile failure and contracture in our studies. This interpretation supports the notion that the onset of outward currents coincides with substantial ATP depletion in intact cells. Another possibility is

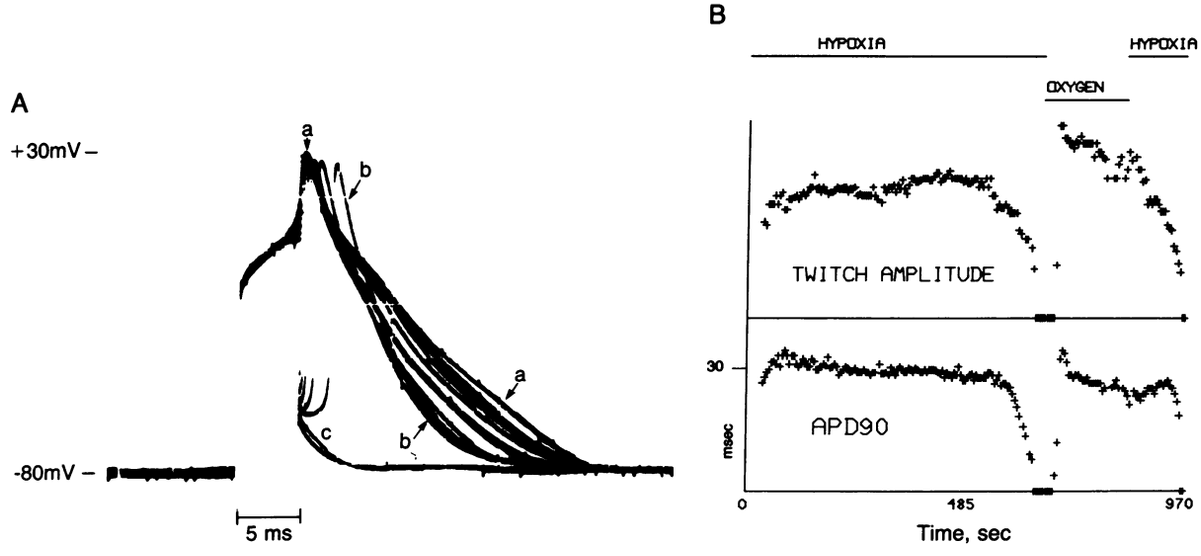

FIG. 5. (*A*) Overlap photograph of action potentials during anoxic contractile failure. Over a 2-min period, control action potentials (trace a) rapidly shorten, then develop increased latency (trace b), and finally fail, leaving subthreshold responses (trace c), the time constant of which continues to decrease. (*B*) Contraction amplitude and action potential duration (at 90% repolarization) (APD90) of a rat myocyte during anoxia, reoxygenation, and a second anoxic period. All action potentials were recorded under current clamp (i.e., current was abruptly clamped to zero, simulating an infinite input-resistance voltage-measuring pipette except during the stimulus, which was a 5-msec injection of depolarizing current).

that a metabolic product that accumulates during hypoxia, perhaps AMP or ADP, competes with ATP at the site of regulation of potassium channels.

The absence of any significant depression of contraction from myofilament-sensitivity decrease early in anoxia, which has been seen in isometric papillary muscles, was initially surprising. This depression is largely attributed to inorganic phosphate accumulation (4). Phosphate depresses *isometric* force in myofilaments, but it accelerates crossbridge turnover and exerts no net effect on the velocity of isotonic shortening (21). It is, therefore, not unexpected that the extent of shortening of myocytes, which are not externally mechanically loaded, would not be decreased. In fact, we observed increases in the velocities of both contraction and relaxation early in anoxia (data not shown).

The laminar counterflow barrier technique permits direct manipulation of single cells under conditions of effective anoxia, which previously could be achieved only with closed systems in which cell access was very limited (10, 22). We anticipate that this technique will find wide application in the study of other cell types and small preparations under conditions of controlled atmosphere.

1. Nayler, W. G., Poole-Wilson, P. A. & Williams, A. (1979) *J. Mol. Cell. Cardiol.* **11**, 683–706.
2. Vleugels, A., Vereecke, J. & Carmeliet, E. (1980) *Circ. Res.* **47**, 501–508.
3. McDonald, T. F. & MacLeod, D. P. (1973) *J. Physiol. (London)* **229**, 559–582.
4. Allen, D. G. & Orchard, C. H. (1987) *Circ. Res.* **60**, 153–168.
5. Barry, W. H., Pober, J., Marsh, J. D., Frankel, S. R. & Smith, T. W. (1980) *Am. J. Physiol.* **239**, H651–H657.
6. Doorey, A. J. & Barry, W. H. (1983) *Circ. Res.* **53**, 192–201.
7. Murphy, J. G., Smith, T. W. & Marsh, J. D. (1987) *J. Mol. Cell. Cardiol.* **19**, 271–279.
8. Hearse, D. J., Humphrey, S. M., Nayler, W. G., Slade, A. & Border, D. (1975) *J. Mol. Cell. Cardiol.* **7**, 315–324.
9. Haworth, R. A. & Berkoff, H. A. (1986) *Circ. Res.* **58**, 157–165.
10. Stern, M. D., Chien, A. M., Capogrossi, M. C., Pelto, D. J. & Lakatta, E. F. (1985) *Circ. Res.* **56**, 899–903.
11. Wojtczak, J. (1979) *Circ. Res.* **44**, 88–95.
12. Wittenberg, B. A. & Wittenberg, J. B. (1985) *J. Biol. Chem.* **260**, 6548–6554.
13. Van der Heyden, G., Vereecke, J., Isenberg, G., Callewaert, G. & Carmeliet, E. (1983) *Arch. Int. Pharmacodyn. Ther.* **263**, 331–332.
14. Bird, R. B., Stewart, W. E. & Lightfoot, E. N. (1960) *Transport Phenomena* (Wiley, New York), p. 503.
15. Poenie, M., Alderton, J., Steinhardt, R. & Tsien, R. W. (1986) *Science* **233**, 886–889.
16. Spurgeon, H. A., Baartz, G., Capogrossi, M. C., Raphaeli, S., Stern, M. D. & Lakatta, E. G. (1988) in *Biology of Isolated Adult Cardiac Myocytes*, eds. Clark, W. A., Decker, R. S. & Borg, P. K. (Elsevier, New York), pp. 350–353.
17. Kammermeier, H., Schmidt, P. & Jungling, E. (1982) *J. Mol. Cell. Cardiol.* **14**, 267–277.
18. Kakei, M., Noma, A. & Shibasaki, T. (1985) *J. Physiol. (London)* **363**, 441–462.
19. Isenberg, G., Vereecke, J., Van der Heyden, G. & Carmeliet, E. (1983) *Pflügers Arch.* **397**, 251–259.
20. Noma, A. & Shibasaki, T. (1985) *J. Physiol. (London)* **363**, 463–480.
21. Kawai, M., Guth, K., Winnikes, K., Haist, C. & Ruegg, J. C. (1987) *Pflügers Arch.* **408**, 1–9.
22. Allshire, A., Piper, H. M., Cuthbertson, K. S. R. & Cobbold, P. H. (1987) *Biochem. J.* **244**, 381–385.